

Article

Modeling of Chloride Binding Capacity in Cementitious Matrices Including Supplementary Cementitious Materials

Ahmed M. Abd El Fattah ^{1,2,*}  and Ibrahim N. A. Al-Duais ³ 

¹ Architecture Department, King Fahd University of Petroleum and Minerals, P.O. Box 215, Dhahran 31261, Saudi Arabia

² Interdisciplinary Research Center for Construction and Building Materials, King Fahd University of Petroleum and Minerals, Dhahran 31261, Saudi Arabia

³ Civil Engineering Department, King Fahd University of Petroleum and Minerals, Dhahran 31261, Saudi Arabia; g200927910@kfupm.edu.sa

* Correspondence: ahmedmohsen@kfupm.edu.sa

Abstract: The improvement in the chloride binding capacity of concrete has been shown to increase corrosion resistance. The addition of supplementary cementitious materials (SCMs) to Portland cement has been proven to increase the binding capacity, except for silica fume, whereas the impact of chemical additives is not extensively addressed in the literature. This work studies the influence of SCMs and chemical additives, i.e., calcium nitrite inhibitor (CNI), migrating corrosion inhibitor (MCI), and Caltite as a hydrophobic material, on binding capacity. The addition of both corrosion inhibitors (MCI and CNI) has minimal effect on the binding capacity, while the addition of Caltite reduces the binding capacity by limiting the contact of the samples with the salt in water due to its hydrophobic nature. In addition, the study compares the performance of the available fitting–binding models against the available experimental work in the literature, and shows that the Freundlich isotherm is the best fitting model for describing the relationship between the binding capacity and the free chloride. The study further relates the binding capacity to different compositions in cement and SCMs, and shows, by conducting quantitative analysis, that the Al_2O_3 content is the dominant factor affecting the binding capacity. Finally, this work proposes a new model, which uses Al_2O_3 content and free salt concentration to predict the bound chloride. The model shows adequate correlations to the experimental work and, further, can be used in service-life modeling of concrete.

Keywords: chloride binding capacity; supplementary cementitious materials; modeling



Citation: Abd El Fattah, A.M.; Al-Duais, I.N.A. Modeling of Chloride Binding Capacity in Cementitious Matrices Including Supplementary Cementitious Materials. *Crystals* **2022**, *12*, 153. <https://doi.org/10.3390/cryst12020153>

Academic Editors: Assem Barakat and Alexander S. Novikov

Received: 29 December 2021

Accepted: 19 January 2022

Published: 21 January 2022

Publisher's Note: MDPI stays neutral with regard to jurisdictional claims in published maps and institutional affiliations.



Copyright: © 2022 by the authors. Licensee MDPI, Basel, Switzerland. This article is an open access article distributed under the terms and conditions of the Creative Commons Attribution (CC BY) license (<https://creativecommons.org/licenses/by/4.0/>).

1. Introduction

Reinforced concrete is one of the major fabricated construction materials that is widely used throughout the globe. Chloride-induced corrosion is the leading cause of deterioration in reinforced concrete and has been the major focus of numerous studies in the literature. Some addressed the time needed for starting corrosion [1,2]. Others showed the influence of supplementary cementitious materials (SCMs) on chloride diffusion [3–6], whereas other studies focused on the impact of marine harsh environments on chloride diffusion [7–10]. Chloride migration through concrete has been explained by multiple literary sources [11–13] as the process in which chloride travels under a concentration differential from higher concentration at the surface of the concrete towards lower concentrations deeper below the surface. This diffusion process is assumed to follow Fick's laws of diffusion [14,15]. When the concentration of chloride ions reaches a certain threshold [11,16], the iron atoms in the reinforcement are activated and react with the chloride ions to form ferrous chloride, which then reacts with water to form ferrous hydroxide, thus regenerating the chloride ions, which become available and are able to react with more iron, leading to further corrosion.

Chloride exists in concrete in two main forms, namely, free chloride and bound chloride. Bound chlorides are chloride ions fixed on cement hydrates and do not move in

the pore solution [17]. They exist as chemically bound and physically bound chloride [18,19]. The process of chemical–chloride binding occurs mainly when tri-calcium aluminate (C_3A) or its hydration products react with chloride ions to form complex alumina-chloride salts such as Friedel’s salt ($C_3A \cdot CaCl_2H_{10}$), calcium mono-chloro-aluminate, or its high-iron analog ($C_3F \cdot CaCl_2H_{10}$) which forms at lower temperatures and in the presence of C_4AF , as Csizmadia et al. explained [20]. Physical binding occurs when chlorides are adsorbed to the surface of C-S-H [19], a process that is dependent on the electrical charges of the different elements and the surface area of the calcium silicate hydrate C-S-H.

Improvements in the chloride-binding capacity (binding capacity) of concrete have been shown to increase corrosion resistance [4]. The main factors that influence the binding capacity include media pH, chloride concentration in the pore solution, the amount of C_3A within the concrete, amount of alkalis and sulfates, associated cation with the chloride ions, and the temperature of the environment [20–25]. Studies have shown that increasing C_3A , as well as the alumina content, improves the binding capacity [8,19]. The increase in the calcium-to-silica ratio will likely lead to a higher binding capacity, especially with the presence of silica fume. In the presence of sulfates, C_3A and its hydration products prefer to react with sulfate to form ettringite; then after exhausting the sulfates, Friedel’s salt formulates [8]. Contrary to common belief, the water-to-binder ratio has been shown to have no influence on the chloride-binding isotherm if the bound chloride is expressed as a fraction of the weight of the C-S-H gel [26,27]. Furthermore, the addition of SCMs to ordinary Portland cement (OPC) has been studied in the literature. SCMs mainly refine pore structure and reduce permeability and ionic diffusivity. The addition of slag cement, referred to in this paper as SC, and fly ash, FA, has been shown to significantly increase the binding capacity even at higher replacement percentages for SC [28,29] because alumina-rich SCMs intensify the formation of Friedel’s salt, and thus increase chloride binding [19]. On the other hand, the addition of silica fume, SF, has been shown to reduce the binding capacity, especially at higher replacement percentages [30] due to the increase in silica content, which changes the physical and chemical properties of C-S-H. The majority of work in the literature studied the impact of specific parameters such as calcium-to-alumina or calcium-to-silica ratios on chloride binding by analyzing a small range of data. Thus, the literature lacks studies that address the simultaneous effects of different parameters on larger data sets.

Besides SCMs, the concrete industry uses chemical additives extensively to enhance different properties of concrete. Corrosion inhibitors contribute to reducing steel corrosion by forming a coating around steel, whereas hydrophobic additives serve as a water repellent and reverse the capillary suction. Chemical additives change the pore structure by introducing different ions, and they sometimes move slowly in the concrete mix to the steel rebar locations. Thus, they might influence the binding capacity [4]. The effect of the chemical additives on the binding is not sufficiently addressed in the literature.

Chloride-binding isotherm models, i.e., mathematical models that relate the binding to free chloride, are fit models that correlate the results to the inputs through fitting parameters. These models can be classified as linear models, such as the Tuutti model, and non-linear models, such as the Langmuir model and the Freundlich model. The linear relationship between bound and free chlorides suggested by linear models is only true for low free-chloride concentrations. When free chloride approaches high molarity, the relation becomes non-linear, so the bound chloride rate decreases to approach maturity level. The Langmuir model has a zero-slope curve at high chloride concentration, whereas the slope of the Freundlich model decreases as the free chloride molarity increases, but the relationship is always ascending. It is noteworthy that all of the available models in the literature do not predict bound chlorides; however, they are used to find a relation between bound and free chlorides.

This study investigates the binding capacity of different mixes that contain SCMs (SC, SF, and FA) and chemical admixtures (calcium nitrite inhibitor (CNI), migrating corrosion inhibitor (MCI), and Caltite, as a hydrophobic material) at different free chloride concen-

trations. The paper further uses the results of binding, alongside the experimental data available in the literature, and quantitatively studies the influence of different parameters, mainly the oxide composition ratios, on the binding capacity and the performance of different available models from the literature. Finally, the study proposes a new model to predict the bound chloride, which can be used in the modeling of concrete service life.

2. Materials and Methods

2.1. Materials and Mix Proportioning

Three mixtures used silica fume (SF), slag cement (SC), and fly ash (FA) as SCMs. A standard mixture of OPC and a type V (high sulfate resistance) mixture was used as well. Table 1 provides the chemical composition and physical properties of the SCMs, OPC, and Type V cement. The remaining mixtures contained OPC and chemical admixtures only, which were a calcium nitrite-based admixture (CNI), migration corrosion inhibitor (MCI), and a hydrophilic chemical (Caltite). This study used a water-to-binder ratio (w/b) of 0.4, which represents the recommended ratio for durability, and a reduction in the w/b leads to a lower binding capacity [9]. Table 2 shows the replacement ratios for the SCMs and dosages of the chemical admixtures according to the manufacturers' recommendation. CNI was obtained from Sika, MCI from Cortec Corp, and Caltite from Cementaid. Slag cement replaced 70% of cement by weight in Mix 5, similar to the Mix of the Bahrain causeway. In Mix 4, fly ash was 25% of the total binder, similar to the optimal value reported in the literature to improve the pore structure [31,32]. Silica fume had a replacement percentage of 6% by weight of cement in Mix 3 because studies have reported best performance to be in the range of 6% to 8% [7,27]. CNI and MCI were added to the mixing water at doses of 20 L/m³ and 0.6 L/m³ of the paste's volume, respectively. Finally, Caltite was used as a hydrophobic agent in the last mixture at a dose of 30 L/m³. The doses were chosen according to the recommendation of the manufacturers.

Table 1. Chemical and physical properties of materials.

Chemical and Physical Analysis (%)	OPC	Cement Type V	Silica Fume	Fly Ash	Slag
SiO ₂	20.8	20.97	91	51.47	34.8
Al ₂ O ₃	5.37	3.91	0.53	24.31	13.4
Fe ₂ O ₃	3.32	4.8	4.77	8.87	0.62
TiO ₂			0.01	1.02	
CaO	63.77	64.27	0.83	5.15	43.4
MgO	2.08	1.97	0.47	3.50	5.44
SO ₃	2.63	1.86		0.23	0.34
Others	3.03	2.22	2.39	5.45	2
Loss on Ignition (L.O.I)	1.34	2.16	6.00	0.53	
Insoluble residue (I.R.)	0.39	0.60			0.34
Na ₂ O _{eq}	0.52	0.48			0.56
K ₂ O				1.47	
P ₂ O ₅				0.257	
C ₃ S	53.20	63.84			
C ₂ S	19.50	11.96			
C ₃ A	8.61	2.24			
C ₄ AF	10.10	14.61			
C ₃ AF + 2C ₃ A	27.33	19.09			
Fineness, Air permeability Test (m ² /Kg)	323	315	15000	338	378

Table 2. Mix proportioning.

Mix	W/B	Cement (Kg/m ³)	Water (Kg/m ³)	Silica Fume (Kg/m ³)	Fly Ash (Kg/m ³)	Slag Cement (Kg/m ³)	Notes
I		340	136	-	-	-	Type OP/CEM 1
V		340	136	-	-	-	Type V/ high sulfate-resistant Portland cement
SF		320	136	21	-	-	OP + SF
FA		255	136	-	85	-	OP + FA
SC	0.4	100	136	-	-	240	OP + SC
MCI		340	136	-	-	-	OP + MCI at 0.6 L/m ³ of paste
CNI		340	136	-	-	-	OP + CNI at 20 L/m ³ of paste
Caltite		340	136	-	-	-	Type I + Caltite at 30 L/m ³ of paste

2.2. Samples Preparation and Testing

ASTM does not provide a way to measure the exact binding capacity. It provides a measure of the total chloride (free and bound) or the water-soluble chloride, which contains parts of the free and bound chlorides [33]. One of the reliable methods found in the literature that measures the chloride binding capacity is a test developed by Nilsson and Luping in 1993 [26]. The method tests the binding capacity of pastes and mortars by submerging them in known concentrations of chloride solutions and estimates the binding capacity by calculating the difference between the known concentration and the measured concentration of the solution after exposure. Chloride is bound in two forms: irreversibly bound chloride that reacts with the (C-S-H) gel and reversibly bound chloride that can unbind when the concentration of chloride in the environment surrounding the concrete is decreased [26]. The test showed that with higher concentrations of chloride in the environment, the binding capacity became higher and irreversible with the increase in the chloride concentration [26]. The test can be summarized as follows:

First, cylindrical paste samples were made (75 mm × 150 mm) using deionized water to eliminate any disturbance in the results caused by the chlorides in the mixing water. Next, samples were cured in lime water (saturated solution of Ca(OH)₂) for 14 days in de-aerated containers to avoid any carbonation that acidifies the paste and led to a reduced chloride-binding capacity according to Saillio et al. [34]. Then, the central portion of each sample was wet crushed and ground to pass through No. 100 size mesh. After that, samples were dried in a desiccator with a bed filled with activated silica gel desiccant, treated at 110 °C for one day to ensure it has no moisture content before use, for one week under vacuum pressure. After drying, samples were treated in a desiccator with a relative humidity content of 11% at room temperature for two weeks, using a saturated solution of Lithium Chloride (LiCl) in the bed of the desiccator (Figure 1a). Finally, they were submerged in a salt and lime solution at different NaCl concentrations.

In this study, free-chloride concentrations of 0.1, 0.3, 0.5, 1, and 4.2 Molar (mol/L) were used. A lower free chloride molarity equal to 3 Molar was used for mix SC, 70% slag, to limit the expected bound chloride due to the instrument limitation. The exposure lasted for 14 days to reach the maximum binding capacity [26]. Then, the samples were filtered and the final chloride concentration was measured using a potentiometric titration of the filtrate after dilution against a solution of silver nitrate with a known concentration and a silver/silver chloride reference electrode (Figure 1b).

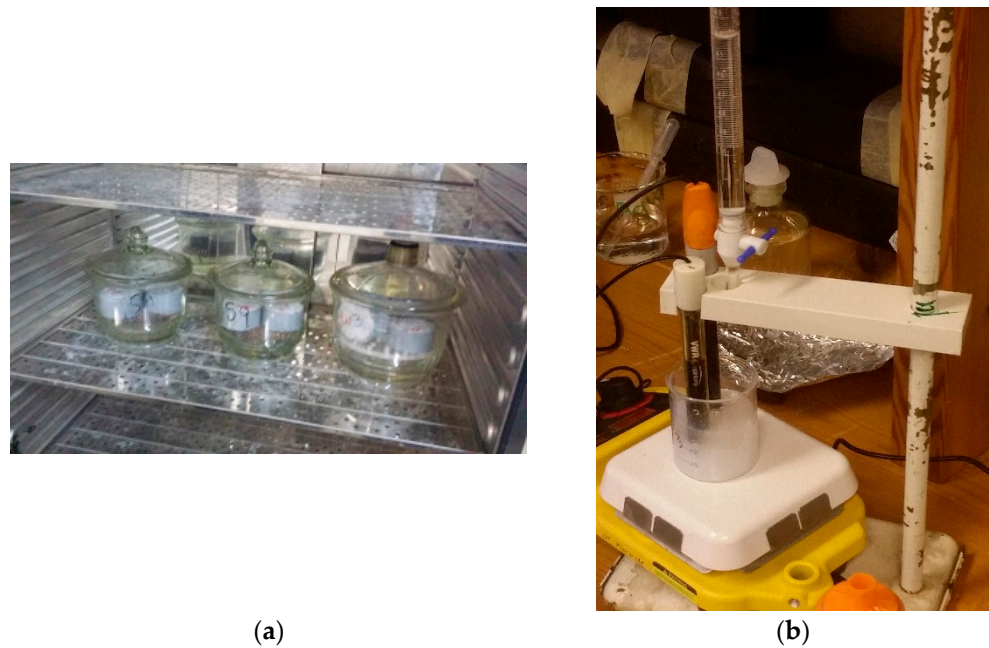


Figure 1. Experimental steps for bound chloride (a) samples' conditioning and (b) potentiometric titration setup.

3. Results and Discussion

As shown in Figure 2, the binding capacity is proportional to the concentration of chloride in the solution. This was exceptionally highlighted in cases of SC and FA pastes, which both exhibited a large increase in the binding capacity with the increase in free chloride in the exposure environment. Their capacities at the highest concentrations increased by 100% and 50%, respectively, compared to Mix I (control mix). Furthermore, SC exhibited the highest binding capacity with increasing concentrations of NaCl in the environment compared to the other mixes. This increase coincides with the reported properties of SC having high alumina and ferric-alumina salts, which help in binding chloride with no reversible mechanism by forming Friedel's salts [10,26,28,35]. This was the case with FA as well, which showed a significant improvement in chloride binding but less than SC overall.

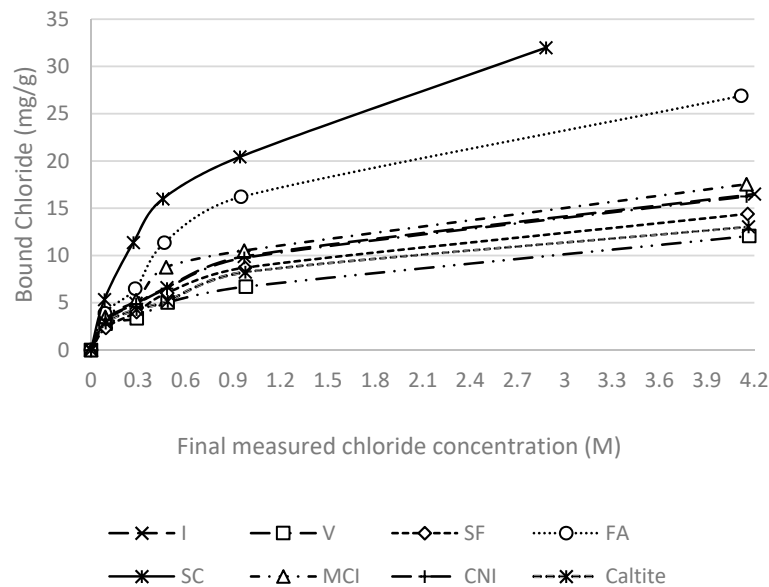


Figure 2. Chloride binding results for the mixes in this study.

On the other hand, Type V cement, as expected, had a low binding capacity due to the lower amount of alumina in the cement compared to Type I cement, as was reported in the literature [27,35,36]. The reduction was consistent at all concentrations, which ranged from 30% to 50%, compared to the control mix. Moreover, the addition of silica fume was shown to negatively impact the binding chloride, which agrees with what was reported by Thomas et al. [9] in pastes with 0.5 w/c, and can be attributed to either the lower amount of alumina and ferric-alumina hydration products or the dilution of C_3A that causes a release of chloride [37]. The addition of CNI and MCI followed the same trend as silica fume in having slight to no effect on the binding properties, especially at higher salt concentrations since their role of inhibiting corrosion has minimal effect on the hydration process and hydration results. Finally, Caltite was shown to reduce the binding significantly, especially at higher concentrations of chloride in the environment, which can be owed to the hydrophobic nature of concretes containing it, which limits the contact between hydration products and chloride, and thus reduces the chance of binding chloride in the first place.

In terms of the relative performances of the mixes compared to each other, SC was shown to have the best binding results out of all the mixes at all environmental salt concentrations, followed by FA as illustrated in Figure 3. Type V, SF, and Caltite had the lowest binding capacity overall compared to the other mixes. CNI and MCI did not show a pronounced difference from Mix I, and finally, FA and SC showed the highest binding capacities.

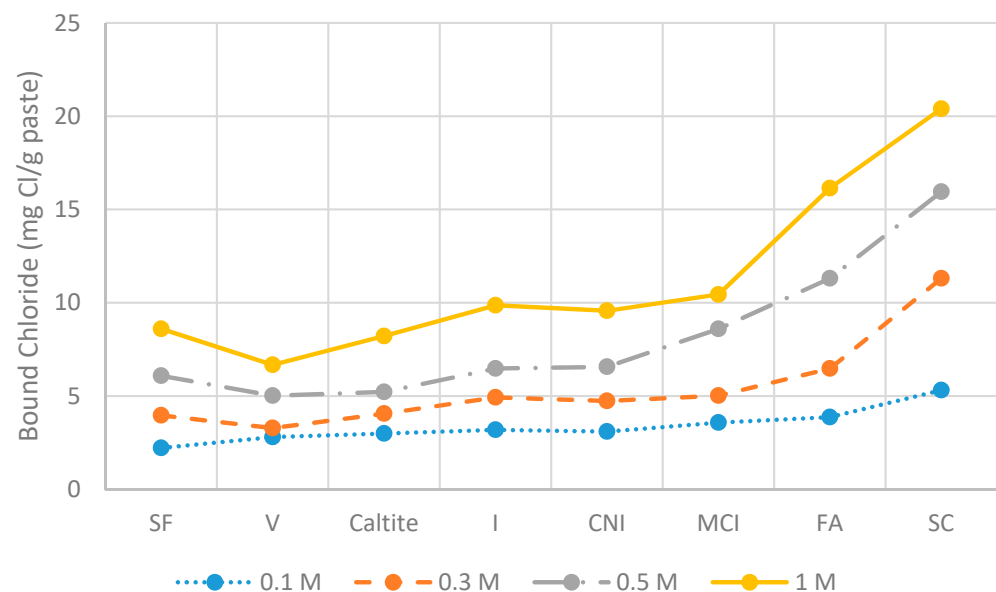


Figure 3. Overall performance of the mixes at each free chloride concentration.

4. Modeling of Chloride Binding

4.1. Available Binding Models

There are several models in the literature that express the chloride-binding phenomenon as a relationship between the bound and free chloride. As previously mentioned, none of the available models in the literature predict the bound chloride; instead, they find a relationship between experimental values of bound and free chlorides through curve fitting constants α and β , whose values differ according to experimental results.

First, the Freundlich isotherm, which is an exponential model, is expressed as

$$C_b = \alpha C_f^\beta. \quad (1)$$

where C_b and C_f are the bound and free chloride, respectively, and α and β are binding constants. Second, the Langmuir model, which is a non-linear model, is expressed as

$$C_b = \frac{\alpha C_f}{(1 + \beta C_f)} \tag{2}$$

where α and β are constants as explained by Luping and Nilsson [26]. Third, the Tuutti linear model [38] is expressed as

$$C_b = \alpha C_f \tag{3}$$

where α is the slope of the binding curve. Fourth, the modified Tuutti model, was suggested by Arya et al. [36] and expressed as

$$C_b = \alpha C_f + \beta \tag{4}$$

where α is the slope of the curve and β is the y -intercept. Figure 4 illustrates the performance of the four models against two experimental mixes, and Table 3 and Figure 5 show the statistical performance of the four models.

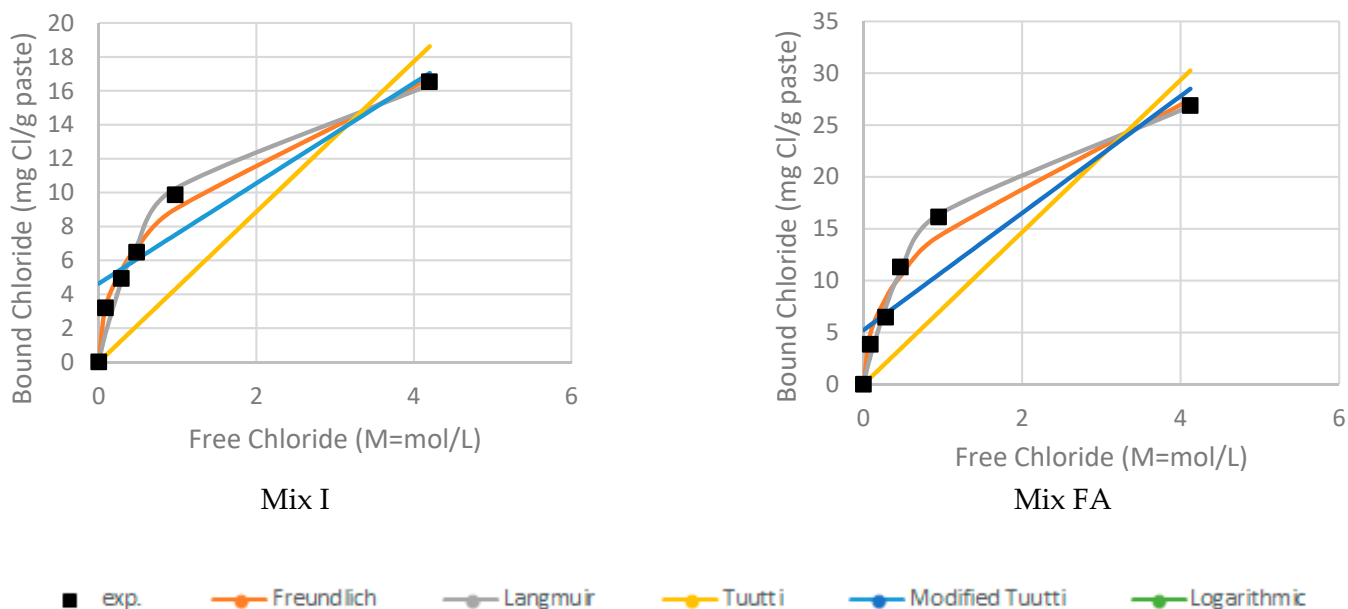


Figure 4. Graphical representation of the binding models against the experimental data.

Table 3. Summary of the regression results for the binding models and the mixes that were used in this study.

M	Langmuir R ²	Freundlich R ²	Tuutti R ²	Modified Tuutti R ²
I	0.979	0.991	0.373	0.924
V	0.963	0.993	0.554	0.865
SF	0.996	0.988	0.574	0.839
FA	0.994	0.981	0.600	0.838
SC	0.990	0.991	0.570	0.837
CNI	0.984	0.987	0.448	0.810
MCI	0.989	0.995	0.552	0.848
Caltite	0.988	0.990	0.472	0.824
β coeff.	0.979	0.983	0.791	0.967

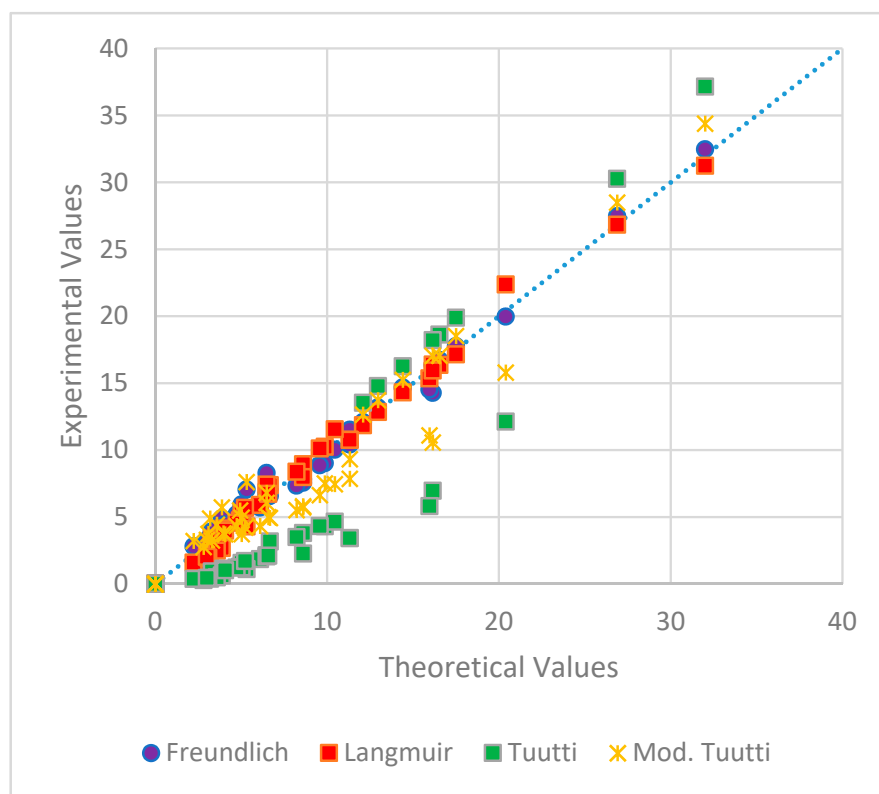


Figure 5. Linear regression analysis of the theoretical versus experimental results.

The Freundlich isotherm showed the best fit to the experimental data, followed by the Langmuir model. The worst fit for a model was found for the Tuutti's model, owing to the linearity of the model.

At concentrations higher than 0.5 Molar, the Langmuir isotherm seems to correlate less and produces results that are further away from the actual data, while linear models seem to fit the data the least. This conclusion agrees with what was reported by Luping and Nilsson [26] regarding the Freundlich, Langmuir, and Tuutti models and disagrees with Mohammed and Hamada [39], who reported a linear relationship between the free and bound chloride. A statistical linear-regression analysis also corroborated the same ranking of the models' performance, with the Freundlich model yielding the highest β coefficient, implying the best performance.

Besides the experimental cases in this study, thirty-two data sets from the literature, detailed in Table 4, were used in regression analysis. The linear models are the most inconsistent, especially for data that have a wider range of free chloride concentration, while the Freundlich and Langmuir models are more consistent and produce less variance as shown in Table 5. The linear regression, Figure 6, supported the superior performance of the Freundlich model, which had β -coefficient and standard error equal to 0.996 and 0.0042, respectively. The β -coefficients are similar for the Langmuir and modified Tuutti models; however, the standard error of modified Tuutti is higher.

Overall, the Freundlich model has more stability, thus, representing the relationship between the bound and free chloride much better than the other models considered in this study.

Table 4. Experimental results from the literature.

Ref	Material	Cement Properties						SCM Properties			
		C3S	C2S	C3A	C4AF	CaO	Al ₂ O ₃	SiO ₂	CaO	Al ₂ O ₃	SiO ₂
[17]	I	57.6	17.6	8.8	5.9	63.58	4.09	21.3	0	0	0
	I + 25% FA	57.6	17.6	8.8	5.9	63.58	4.09	21.3	4.37	20.78	53.89
[40]	I + 30%SC	62.1	8.9	8.5	9.1	62.38	5.89	19.1	38.24	12.23	36.58
[26]	I	61.91	10.42	8.55	8.52	62.1	5.3	19.9	0	0	0
[27]	I	68.7	5.9	7.4	5.1	63.8	3.9	20.1	0	0	0
	V	54.9	22.5	1.8	13.3	63.9	3.5	22.3	0	0	0
[41]	I + 68% SC	68.4	4.5	8.3	8.9	62.53	4.98	19.5	48.4	13.4	34.8
[34]	I	51.23	28.32	9.9	8.81	62.53	4.98	19.5	0	0	0
	I + 30% FA	51.23	28.32	9.9	8.81	62.53	4.98	19.5	0	23.78	51.59
[42]	I	70.83	5.93	7.12	9.13	64.7	4.6	20.7	0	0	0
	I + 30% FA	70.83	5.93	7.12	9.13	64.7	4.6	20.7	1.7	18.8	48.7
	I + 60% SC	70.83	5.93	7.12	9.13	64.7	4.6	20.7	44.2	11.7	34.2
[43]	I	68.98	3.1	7.9	9.1	61.83	4.84	19.2	0	0	0
[44]	I	78.86	3.7	7.1	8.7	63.996	4.456	19.4	0	0	0
[45]	I	78.45	6.1	12.1	8.9	65.4	6.4	18.5	0	0	0
[30]	I	62.1	15.1	6.6	9.1	63.81	4.35	21.6	0	0	0
	I + 4% SF	62.1	15.1	6.6	9.1	63.81	4.35	21.6	0.44	0.18	95.11
[46]	I	70.83	6.0	7.2	9.2	64.7	4.6	20.7	0	0	0
	I + 10% SF	70.83	6.0	7.2	9.2	64.7	4.6	20.7	0.31	0.23	94.9
[9]	I	57.6	17.6	5.9	8.8	63.58	4.09	21.3	0	0	0
	I + 8% SF	57.6	17.6	5.9	8.8	63.58	4.09	21.3	0.44	0.24	94.48
	I + 25% SC	57.6	17.6	5.9	8.8	63.58	4.09	21.3	35.49	10.02	36.18
	I + 25% FA	57.6	17.6	5.9	8.8	63.58	4.09	21.3	4.37	24.65	53.89
[47]	I	53.83	22.8	8.2	9.2	63.8	5.0	22.1	0	0	0
[48]	I	60.71	14.7	2.2	13.7	61.93	3.69	21.1	0	0	0
	I + 10% SF	60.71	14.7	2.2	13.7	61.93	3.69	21.1	0.56	0.03	94.92
	I + 20% FA	60.71	14.7	2.2	13.7	61.93	3.69	21.1	4.68	20.38	62.28
[49]	I	36.73	34	10.9	8.5	59.82	5.86	21.5	0	0	0
[50]	I	61	8.0	9.0	10	63.4	4.6	20.2	0	0	0

Table 5. Descriptive analysis of the Coefficient of Determination for the data gathered from the literature as well as the data in this paper.

	Freundlich	Langmuir	Tuutti	Mod. Tuutti
Mean	0.971	0.952	0.439	0.895
Median	0.982	0.963	0.601	0.905
Variance	0.001	0.002	0.251	0.006
Minimum	0.802	0.822	−0.917	0.54
Maximum	0.999	0.999	0.997	1.0
β -coeff.	0.996	0.978	0.90	0.978
Std. Error	0.0042	0.0086	0.0215	0.0106

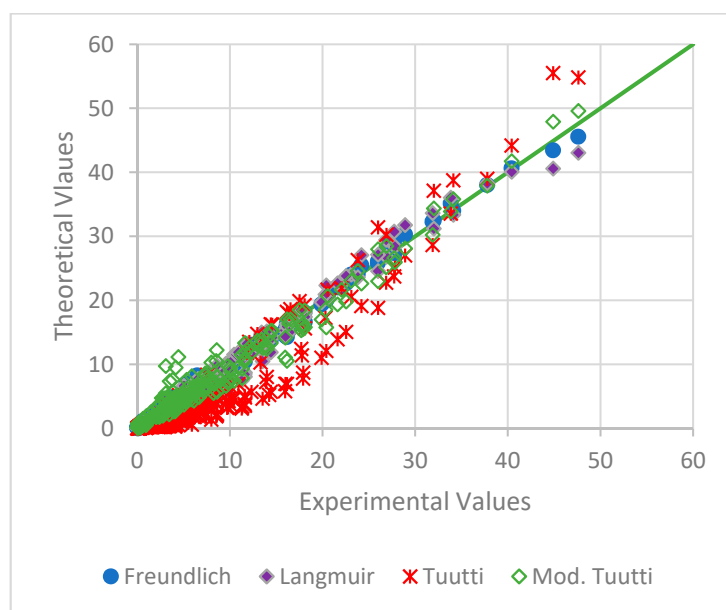


Figure 6. Linear regression analysis of the theoretical versus experimental results in the literature.

4.2. New Model Development

According to the literature, the chemical-oxide compositions of cement, i.e., Al_2O_3 , SiO_2 , and CaO content and their ratios are significant parameters in determining the binding capacity [8,19] because they impact the ratios of calcium, silicate, and alumina in the C-S-H and C-A-S-H. To quantitatively identify the influential trends of the content of the oxides on the binding capacity, the analysis performed here conducts different comparisons: first, a comparison between experimental cases and their control mixes where CaO/SiO_2 is the main changing variable when silica fume is used, or where Al_2O_3 is the main variable when fly ash and slag cement are used. The second comparison is between the bound chloride and different oxide ratios for all of the data gathered in Table 4 and presented in this paper, without isolation of variables to define the most dominant affecting parameters. Figure 7 compares the bound chloride against CaO/SiO_2 for cases in Ref [9,30,46,48], and Mix SF where silica fume is used. Here, the CaO/SiO_2 ratio is the main varying parameter; for instance, Mix SF is compared to its control mix (Mix I) and so forth. Increasing the CaO/SiO_2 ratio increases the bound chloride, and this is in agreement with the literature because even while increasing the silicate, increasing the ratio of CaO/SiO_2 changes the nature and composition of C-S-H gel and causes it to bind less chloride [9,17,18,27]. Only one case reports the opposite, and it is noteworthy that this case is measured using a new untraditional technique [48]. Similarly, in Figure 8, which compares bound chloride to Al_2O_3 content for cases in [9,17,34,45,50] and Mixes SC and FA, where slag cement and fly ash are used, bound chloride values increase with increasing Al_2O_3 content. Only one case reports the opposite, in which the w/c ratio was as little as 0.3. It is worth mentioning that CaO/SiO_2 ratio also decreased because of the SiO_2 content of fly ash and slag cement; however, it did not affect the results. This might imply that the Al_2O_3 content, when present, is the main driving parameter in determining the binding capacity, and CaO/SiO_2 becomes the dominant parameter when Al_2O_3 quantity does not noticeably change, i.e., when silica fume is used.

To confirm the aforementioned statement, Figures 9–14 compare the bound chloride to different oxide contents and ratios, such as SiO_2 , Al_2O_3 , CaO , CaO/SiO_2 , $\text{CaO}/\text{Al}_2\text{O}_3$, and $\text{Al}_2\text{O}_3/\text{SiO}_2$, for different chloride concentration ranges, regardless of other elements' percentages. For illustration, Figure 9 plots the bound chloride versus CaO content of all experimental cases in Table 4 and this study, regardless of the variation of other oxides to capture the dominance of the CaO . The Al_2O_3 content ratio, as opposed to other oxides, shows a persistent proportional tendency with bound chloride to reflect a strong correlation

to binding capacity as the regression analysis shows in Figure 11, complying with [27]. Figures 13 and 14 confirm that even if the ratio of Al_2O_3 changes against CaO or SiO_2 , the trend is still the same as presented in Figure 11. Thomas et al. [9] shows that mixes with metakaolin, which contain almost equal amounts of Al_2O_3 and SiO_2 , have higher binding capacity compared to the control mix, which implies that Al_2O_3 is a dominant factor in determining the binding capacity. This observation cannot be confirmed for the other two oxides that show an inverse relation to CaO at small chloride concentration and direct relationship at higher concentration, i.e., 1.25 Molar or above, as shown in Figure 9. The opposite relationships are observed for SiO_2 in Figure 10. Figure 12 speculates that the CaO/SiO_2 effect becomes pronounced at high chloride concentrations, which agrees with Figure 2 in that the binding curve for Mix SF deviates away from the control mix at a concentration of 1 Molar. Results from the literature are similar to this observation, which might be attributed to the role of Al_2O_3 in binding until it is completely exhausted.

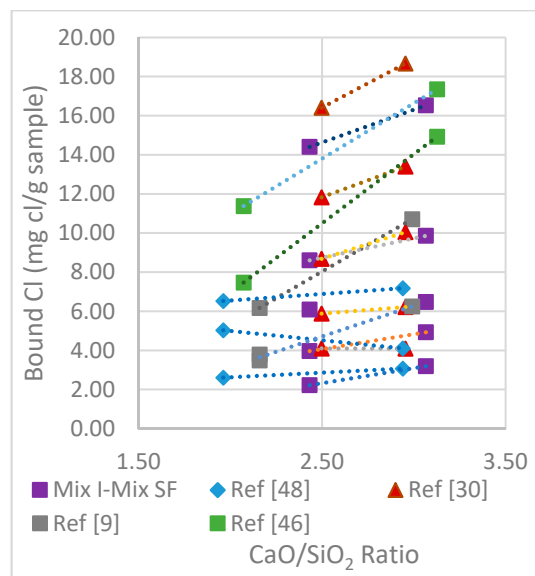


Figure 7. Relationship between CaO/SiO_2 ratio (main varying-parameter) and bound chloride for different chloride concentrations.

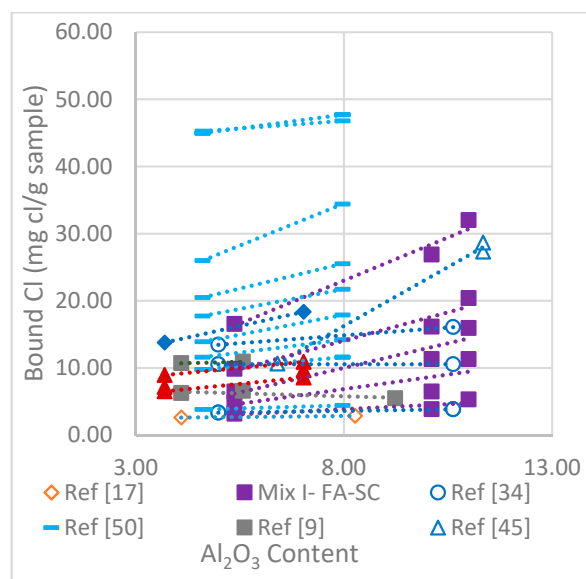


Figure 8. Relationship between Al_2O_3 content ratio and bound chloride for different chloride concentrations.

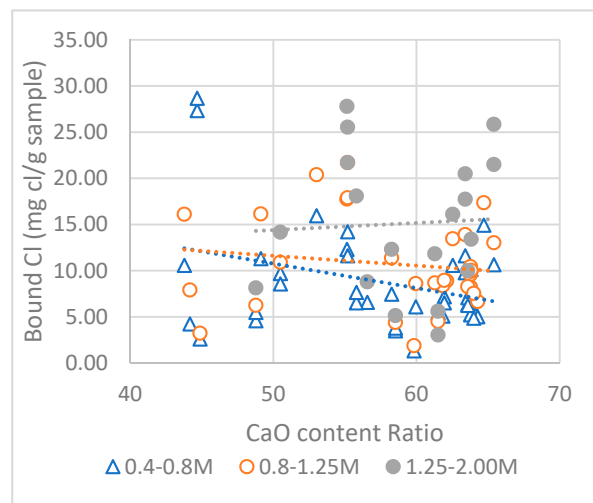


Figure 9. Relation between CaO ratio and bound chloride for different chloride concentrations for all data.

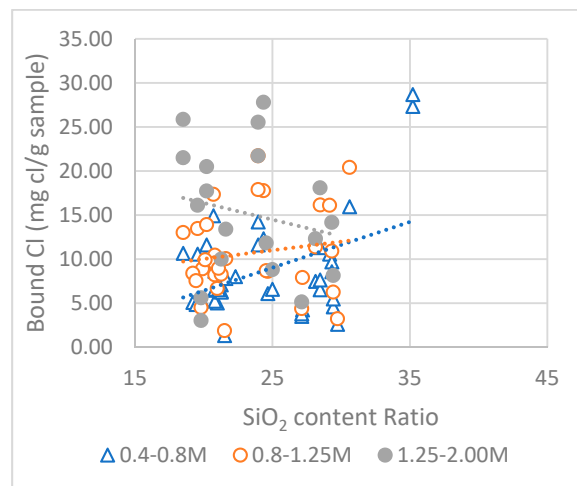


Figure 10. Relation between SiO₂ ratio and bound chloride for different chloride concentrations for all data.

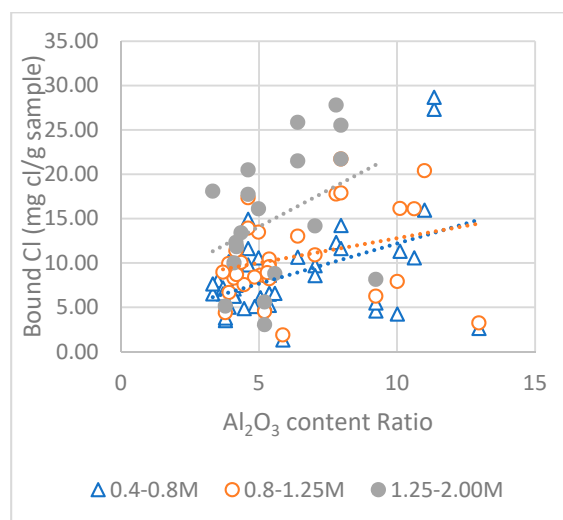


Figure 11. Relation between Al₂O₃ ratio and bound chloride for different chloride concentrations for all data.

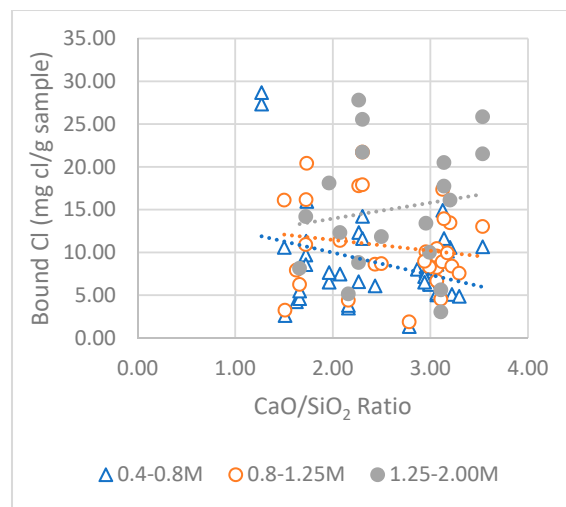


Figure 12. Relation between CaO/SiO₂ ratio and bound chloride for different chloride concentrations for all data.

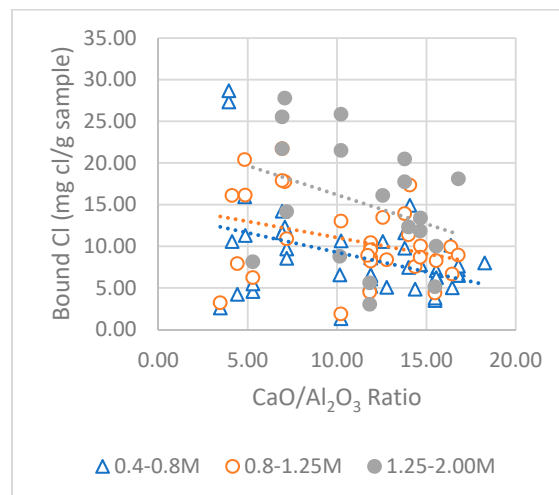


Figure 13. Relation between CaO/Al₂O₃ ratio and bound chloride for different chloride concentrations for all data.

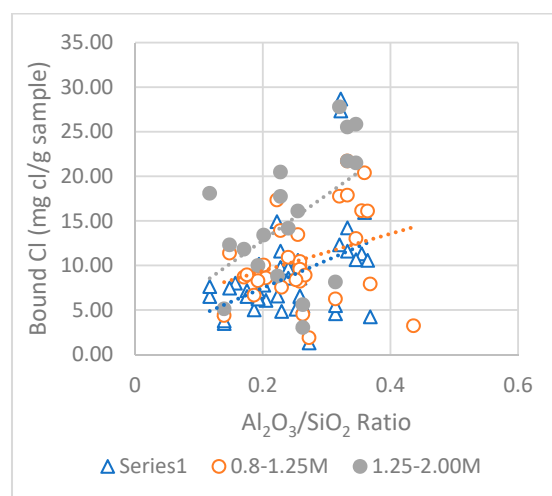


Figure 14. Relation between Al₂O₃/SiO₂ ratio and bound chloride for different chloride concentrations for all data.

For further confirmation, the data in Table 4 are regrouped according to CaO/SiO₂ ratios and Al₂O₃ content, and bound chloride is plotted against the free chloride in Figures 15 and 16, respectively.

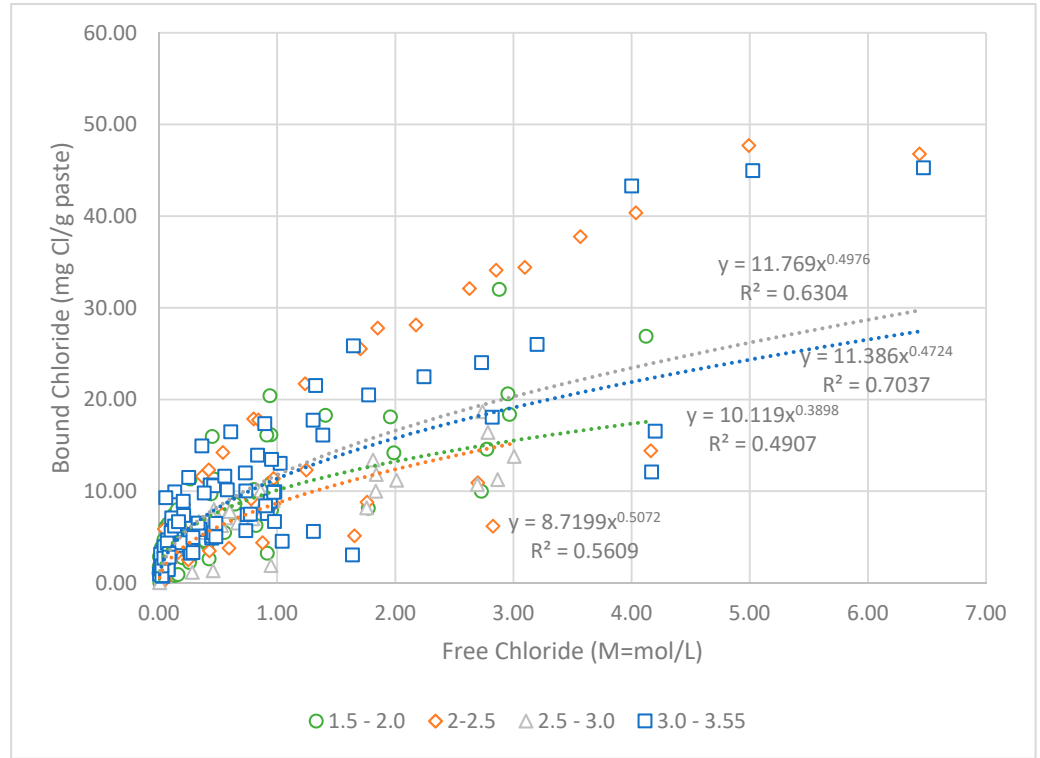


Figure 15. Bound Chloride versus free chloride for different CaO/SiO₂ ratios.

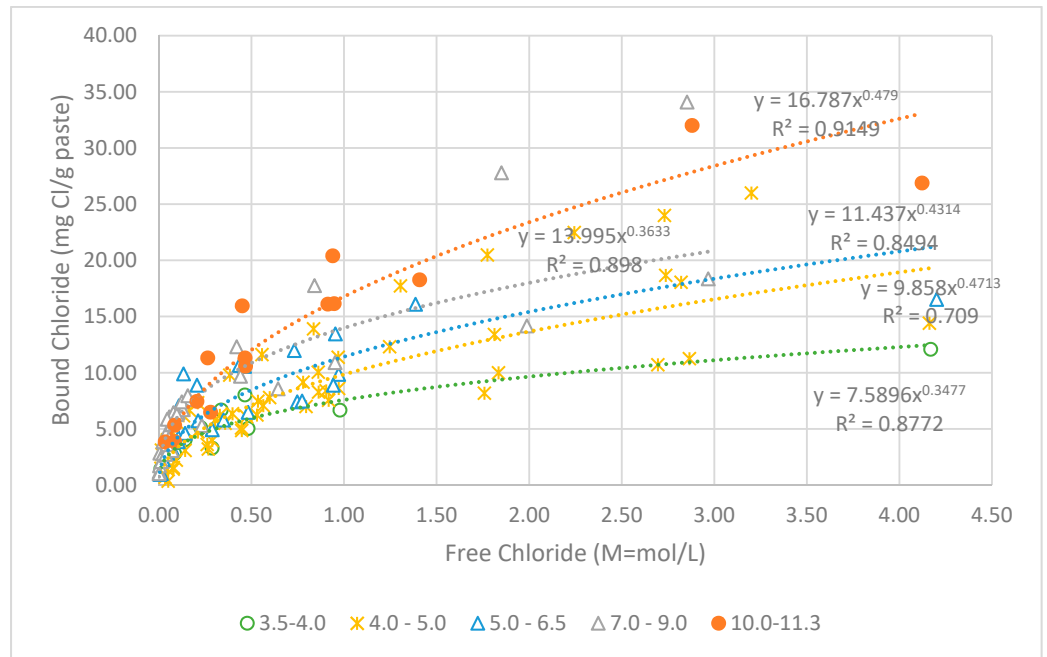


Figure 16. Bound Chloride versus free chloride for different Al₂O₃ content.

It is clear from Figure 16 that increasing the Al₂O₃ content increases the binding capacity, even when other contents in the mixes change, which confirms that the Al₂O₃ content is the main driving parameter. On the contrary, Figure 15 did not evidence the same trend for the CaO/SiO₂ ratio, which might imply that it is a dominant factor only

when it is the main varying parameter, such as in cases with silica fume. Based on Figure 16 and by conducting a regression analysis, α and β relate to Al_2O_3 content ratio (AC) by the following equations:

$$\alpha = 1.3 AC + 3.44. \tag{5}$$

$$\beta = 0.0077 AC + 0.30 \tag{6}$$

This empirical model solves for α and β in Equations (5) and (6) using AC as an input, and then solves for the bound chloride using the Freundlich relation in Equation (1) using the free chloride value, α , and β .

Figure 17 shows a β coefficient of 0.99 between theoretical values found using the proposed model and experimental values of bound chloride. The correlation between the model and experimental results is 0.834. The T-value is 0.35, which is smaller than the t-critical of 1.964 at a 95% confidence level, and the mean absolute error is 0.15. Figure 18 demonstrates the validity of the proposed model by plotting one case from each Al_2O_3 content group shown in Figure 16. The proposed model has a satisfactory correlation to the experimental data given the wide range of experimental results. Thus, the model can be used in the service life of modeling concrete.

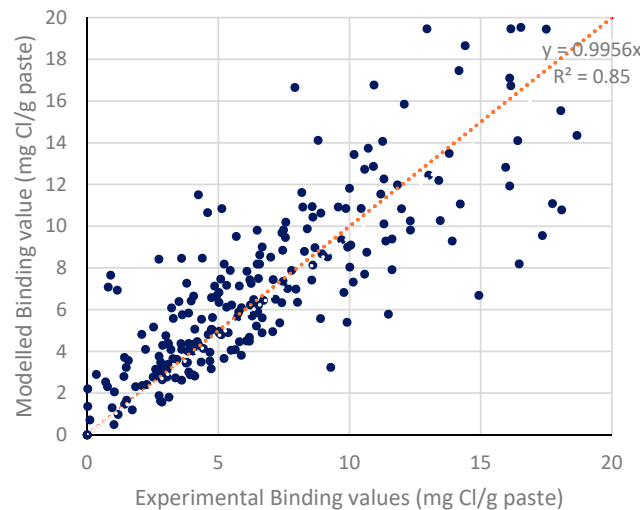


Figure 17. Linear regression analysis of the proposed model versus experimental results in the literature.

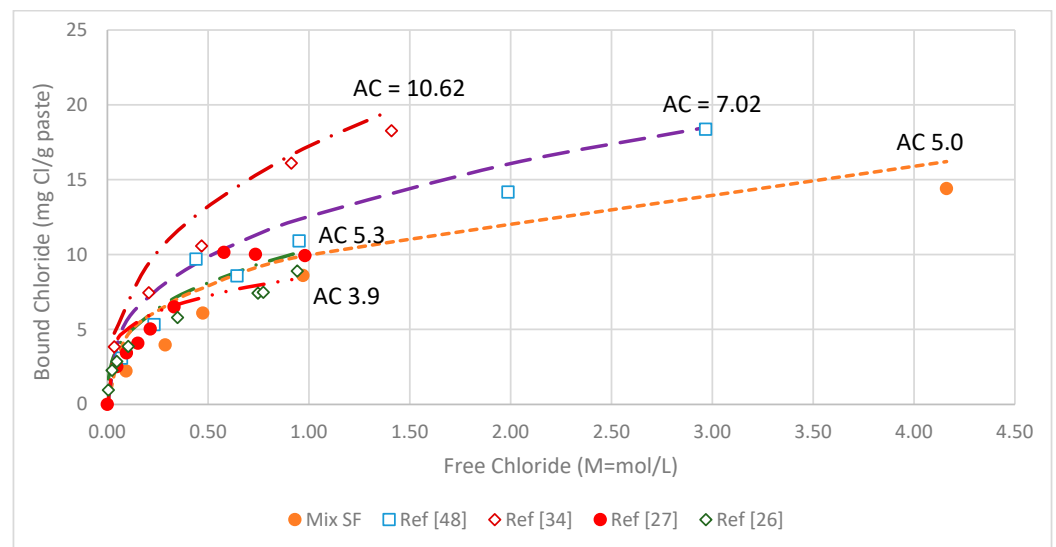


Figure 18. Validation of the proposed model against the experimental cases.

5. Conclusions

In this study, the binding capacity of pastes containing different mineral and chemical admixtures is evaluated using the process developed by Luping and Nilsson at different free-chloride concentrations ranging from 0.1 Molar to 4.2 Molar. In addition, the relationship between binding capacity and free chloride concentration is investigated using four models from the literature. Furthermore, the investigation of the relationship is extended to 36 data sets extracted from the literature. Then, a new model has been proposed that predicts the bound chloride. The conclusions of this study are as follows:

1. Binding capacity significantly improves when using slag cement and fly ash, for the given ratios, with an increase of 100% and 50%, respectively, compared to the control mix.
2. Binding capacity is reduced by 30% to 50% when using SF and Type V cement compared to the control mix.
3. The addition of both corrosion inhibitors (MCI and CNI) has a minimal effect on binding capacity, while the addition of a hydrophobic agent (Caltite) reduces the binding capacity by limiting the contact of the samples with saltwater due to its hydrophobic nature.
4. The Freundlich isotherm performs the best amongst models that are used for describing the relationship between binding capacity and free chloride, and it produces the most consistent results with a variance of less than 0.001 in the coefficient of determination, a mean of 0.971, and a β coefficient value of 0.996.
5. According to the qualitative analysis conducted, Al_2O_3 content is the dominant parameter that consistently defines binding capacity, and can relate to binding capacity in defining a new model.
6. The proposed model predicts bound chloride, based on the concentration of chloride in the environment and Al_2O_3 content in the paste. It proposes new equations for finding α and β , shows good agreement with the experimental work, and, further, can be used as a simple model in the service-life modeling of concrete.

Author Contributions: Conceptualization, A.M.A.E.F.; methodology, A.M.A.E.F.; validation, A.M.A.E.F. and I.N.A.A.-D.; formal analysis, I.N.A.A.-D.; investigation, A.M.A.E.F.; resources, I.N.A.A.-D.; data curation, I.N.A.A.-D.; writing—original draft preparation, A.M.A.E.F. and I.N.A.A.-D. writing—review and editing, A.M.A.E.F.; visualization, I.N.A.A.-D.; supervision, A.M.A.E.F.; project administration, A.M.A.E.F.; funding acquisition, A.M.A.E.F.; All authors have read and agreed to the published version of the manuscript.

Funding: This research was funded by the deanship of scientific research (DSR), grant number IN161050 and the APC was funded by KFUPM.

Data Availability Statement: The data presented in this study is available in the cited journals.

Acknowledgments: The authors acknowledge the support provided by the Deanship of Scientific Research (DSR) at King Fahd University of Petroleum and Minerals (KFUPM) for funding this work through project no. IN161050.

Conflicts of Interest: The authors declare no conflict of interest.

References

1. Ann, K.; Ahn, J.; Ryou, J. The importance of chloride content at the concrete surface in assessing the time to corrosion of steel in concrete structures. *Constr. Build. Mater.* **2009**, *23*, 239–245. [[CrossRef](#)]
2. Nokken, M.; Boddy, A.; Hooton, R.; Thomas, M. Time dependent diffusion in concrete—Three laboratory studies. *Cem. Concr. Res.* **2006**, *36*, 200–207. [[CrossRef](#)]
3. Valipour, M.; Pargar, F.; Shekarchizadeh, M.; Khani, S.; Moradian, M. In situ study of chloride ingress in concretes containing natural zeolite, metakaolin and silica fume exposed to various exposure conditions in a harsh marine environment. *Constr. Build. Mater.* **2013**, *46*, 63–70. [[CrossRef](#)]
4. Abd El Fattah, A.; Al-Duais, I.; Riding, K.; Thomas, M. Field evaluation of corrosion mitigation on reinforced concrete in marine exposure conditions. *Constr. Build. Mater.* **2018**, *165*, 663–674. [[CrossRef](#)]

5. Schueremans, L.; Van Gemert, D.; Giessler, S. Chloride penetration in RC-structures in marine environment—Long term assessment of a preventive hydrophobic treatment. *Constr. Build. Mater.* **2006**, *21*, 1238–1249. [[CrossRef](#)]
6. de Rincón, O.T.; Sánchez, M.; Millano, V.; Fernández, R.; de Partidas, E.; Andrade, C.; Martínez, I.; Castellote, M.; Barboza, M.; Irassar, F.; et al. Effect of the marine environment on reinforced concrete durability in Iberoamerican countries: DURACON project/CYTED. *Corros. Sci.* **2007**, *49*, 2832–2843. [[CrossRef](#)]
7. Hooton, R.D.; Pun, P.; Kojundic, T.; Fidjestol, P. Influence of silica fume on chloride resistance of concrete. In Proceedings of the PCI/FHWA International Symposium of High Performance Concrete, New Orleans, LA, USA, 20–22 October 1997; pp. 245–249.
8. Zibara, H.; Hooton, R.D.; Thomas, M.; Stanish, K. Influence of the C/S and C/A ratios of hydration products on the chloride ion binding capacity of lime-SF and lime-MK mixtures. *Cem. Concr. Res.* **2008**, *38*, 422–426. [[CrossRef](#)]
9. Thomas, M.D.A.; Hooton, R.D.; Scott, A.; Zibara, H. The effect of supplementary cementitious materials on chloride binding in hardened cement paste. *Cem. Concr. Res.* **2012**, *42*, 1–7. [[CrossRef](#)]
10. Bleszynski, R.; Hooton, R.D.; Thomas, M.D.; Rogers, C.A. Durability of ternary blend concrete with silica fume and blast-furnace slag: Laboratory and outdoor exposure site studies. *Mater. J.* **2002**, *99*, 499–508.
11. Neville, A.M. *Properties of Concrete*; Longman: London, UK, 1995; Volume 4.
12. Ma, B.; Liu, X.; Tan, H.; Zhang, T.; Mei, J.; Qi, H.; Jiang, W.; Zou, F. Utilization of pretreated fly ash to enhance the chloride binding capacity of cement-based material. *Constr. Build. Mater.* **2018**, *175*, 726–734. [[CrossRef](#)]
13. Zuquan, J.; Xia, Z.; Tiejun, Z.; Jianqing, L. Chloride ions transportation behavior and binding capacity of concrete exposed to different marine corrosion zones. *Constr. Build. Mater.* **2018**, *177*, 170–183. [[CrossRef](#)]
14. Hodhod, O.; Ahmed, H. Modeling the service life of slag concrete exposed to chlorides. *Ain Shams Eng. J.* **2014**, *5*, 49–54. [[CrossRef](#)]
15. Meng, Q.; Zhang, Y.; Lin, C.-J.; Jiang, L.-H.; Chen, D. Modeling of Chloride Distribution in Cement-Based Materials with Neumann Boundary Condition. *Adv. Mater. Sci. Eng.* **2018**, *2018*, 8085954. [[CrossRef](#)]
16. Thomas, M. Chloride thresholds in marine concrete. *Cem. Concr. Res.* **1996**, *26*, 513–519. [[CrossRef](#)]
17. Zibara, H. *Binding of External Chlorides by Cement Pastes*; University of Toronto: Toronto, ON, Canada, 2001.
18. Ramachandran, V.S. Possible states of chloride in the hydration of tricalcium silicate in the presence of calcium chloride. *Matériaux Constr.* **1971**, *4*, 3–12. [[CrossRef](#)]
19. Dousti, A.; Beaudoin, J.J.; Shekarchi, M. Chloride binding in hydrated MK, SF and natural zeolite-lime mixtures. *Constr. Build. Mater.* **2017**, *154*, 1035–1047. [[CrossRef](#)]
20. Csizmadia, J.; Balázs, G.; Tamás, F.D. Chloride ion binding capacity of aluminoferrites. *Cem. Concr. Res.* **2001**, *31*, 577–588. [[CrossRef](#)]
21. Shakouri, M.; Trejo, D. A study of the factors affecting the surface chloride maximum phenomenon in submerged concrete samples. *Cem. Concr. Compos.* **2018**, *94*, 181–190. [[CrossRef](#)]
22. Trejo, D.; Shakouri, M.; Vaddey, N.P.; Isgor, O.B. Development of empirical models for chloride binding in cementitious systems containing admixed chlorides. *Constr. Build. Mater.* **2018**, *189*, 157–169. [[CrossRef](#)]
23. Ipavec, A.; Vuk, T.; Gabrovšek, R.; Kaučič, V. Chloride binding into hydrated blended cements: The influence of limestone and alkalinity. *Cem. Concr. Res.* **2013**, *48*, 74–85. [[CrossRef](#)]
24. Panesar, D.K.; Chidiac, S.E. Effect of Cold Temperature on the Chloride-Binding Capacity of Cement. *J. Cold Reg. Eng.* **2011**, *25*, 133–144. [[CrossRef](#)]
25. Rasheeduzzafar, Al-Saadoun, S.; Al-Gahtani, A.; Dakhil, F. Effect of tricalcium aluminate content of cement on corrosion of reinforcing steel in concrete. *Cem. Concr. Res.* **1990**, *20*, 723–738. [[CrossRef](#)]
26. Luping, T.; Nilsson, L.-O. Chloride binding capacity and binding isotherms of OPC pastes and mortars. *Cem. Concr. Res.* **1993**, *23*, 247–253. [[CrossRef](#)]
27. Delagrave, A.; Marchand, J.; Ollivier, J.-P.; Julien, S.; Hazrati, K. Chloride binding capacity of various hydrated cement paste systems. *Adv. Cem. Based Mater.* **1997**, *6*, 28–35. [[CrossRef](#)]
28. Cheewaket, T.; Jaturapitakkul, C.; Chalee, W. Long term performance of chloride binding capacity in fly ash concrete in a marine environment. *Constr. Build. Mater.* **2010**, *24*, 1352–1357. [[CrossRef](#)]
29. Luo, R.; Cai, Y.; Wang, C.; Huang, X. Study of chloride binding and diffusion in GGBS concrete. *Cem. Concr. Res.* **2003**, *33*, 1–7. [[CrossRef](#)]
30. Guo, Y.; Zhang, T.; Tian, W.; Wei, J.; Yu, Q. Physically and chemically bound chlorides in hydrated cement pastes: A comparison study of the effects of silica fume and metakaolin. *J. Mater. Sci.* **2018**, *54*, 2152–2169. [[CrossRef](#)]
31. Islam, M.M.; Islam, M.S. Strength and durability characteristics of concrete made with fly-ash blended cement. *Aust. J. Struct. Eng.* **2013**, *14*, 303–319. [[CrossRef](#)]
32. Dhir, R.; El-Mohr, M.; Dyer, T. Developing chloride resisting concrete using PFA. *Cem. Concr. Res.* **1997**, *27*, 1633–1639. [[CrossRef](#)]
33. Haque, M.; Kayyali, O. Free and water soluble chloride in concrete. *Cem. Concr. Res.* **1995**, *25*, 531–542. [[CrossRef](#)]
34. Saillio, M.; Baroghel-Bouny, V.; Barberon, F. Chloride binding in sound and carbonated cementitious materials with various types of binder. *Constr. Build. Mater.* **2014**, *68*, 82–91. [[CrossRef](#)]
35. Florea, M.V.A.; Brouwers, H.J.H. Chloride binding related to hydration products: Part I: Ordinary Portland Cement. *Cem. Concr. Res.* **2012**, *42*, 282–290. [[CrossRef](#)]

36. Arya, C.; Buenfeld, N.R.; Newman, J.B. Factors influencing chloride-binding in concrete. *Cem. Concr. Res.* **1990**, *20*, 291–300. [[CrossRef](#)]
37. Dousti, A.; Shekarchi, M.; Alizadeh, R.; Taheri-Motlagh, A. Binding of externally supplied chlorides in micro silica concrete under field exposure conditions. *Cem. Concr. Compos.* **2011**, *33*, 1071–1079. [[CrossRef](#)]
38. Tuutti, K. Analysis of pore solution squeezed out of cement paste and mortar. *Nord. Concr. Res.* **1982**, *1*, 1–16.
39. Mohammed, T.; Hamada, H. Relationship between free chloride and total chloride contents in concrete. *Cem. Concr. Res.* **2003**, *33*, 1487–1490. [[CrossRef](#)]
40. Ogrigbo, O.R.; Black, L. Chloride binding and diffusion in slag blends: Influence of slag composition and temperature. *Constr. Build. Mater.* **2017**, *149*, 816–825. [[CrossRef](#)]
41. Saillio, M.; Baroghel-Bouny, V.; Pradelle, S. Effect of Carbonation and Sulphate on Chloride Ingress in Cement Pastes and Concretes with Supplementary Cementitious Materials. *Key Eng. Mater.* **2016**, *711*, 241–248. [[CrossRef](#)]
42. Song, H.W.; Lee, C.H.; Jung, M.S.; Ann, K.Y. Development of chloride binding capacity in cement pastes and influence of the pH of hydration products. *Can. J. Civ. Eng.* **2008**, *35*, 1427–1434. [[CrossRef](#)]
43. Moffatt, E.T.G.; Thomas, M.D. Effect of Carbonation on the Durability and Mechanical Performance of Ettringite-Based Binders. *ACI Mater. J.* **2019**, *116*, 95–102. [[CrossRef](#)]
44. Yang, Z.; Gao, Y.; Mu, S.; Chang, H.; Sun, W.; Jiang, J. Improving the chloride binding capacity of cement paste by adding nano- Al_2O_3 . *Constr. Build. Mater.* **2018**, *195*, 415–422. [[CrossRef](#)]
45. Ann, K.Y.; Hong, S.I. Modeling Chloride Transport in Concrete at Pore and Chloride Binding. *ACI Mater. J.* **2018**, *115*. [[CrossRef](#)]
46. Jung, M.S.; Kim, K.B.; Lee, S.A.; Ann, K.Y. Risk of chloride-induced corrosion of steel in SF concrete exposed to a chloride-bearing environment. *Constr. Build. Mater.* **2018**, *166*, 413–422. [[CrossRef](#)]
47. Ann, K.; Kim, T.-S.; Kim, J.; Kim, S.-H. The resistance of high alumina cement against corrosion of steel in concrete. *Constr. Build. Mater.* **2010**, *24*, 1502–1510. [[CrossRef](#)]
48. Ramírez-Ortíz, A.E.; Castellanos, F.; Cano-Barrita, P.F.D.J. Ultrasonic Detection of Chloride Ions and Chloride Binding in Portland Cement Pastes. *Int. J. Concr. Struct. Mater.* **2018**, *12*, 20. [[CrossRef](#)]
49. Wang, Y.; Shui, Z.; Gao, X.; Yu, R.; Huang, Y.; Cheng, S. Understanding the chloride binding and diffusion behaviors of marine concrete based on Portland limestone cement-alumina enriched pozzolans. *Constr. Build. Mater.* **2019**, *198*, 207–217. [[CrossRef](#)]
50. Qiao, C.; Suraneni, P.; Ying, T.N.W.; Choudhary, A.; Weiss, J. Chloride binding of cement pastes with fly ash exposed to CaCl_2 solutions at 5 and 23 °C. *Cem. Concr. Compos.* **2019**, *97*, 43–53. [[CrossRef](#)]